ChemComm

COMMUNICATION

Efficient PdNi and PdNi@Pd-catalyzed hydrogen generation *via* formic acid decomposition at room temperature†

Yu-ling Qin,[ab] Jun Wang,[ab] Fan-zhi Meng,[a] Li-min Wang[ac] and Xin-bo Zhang*[a]

Formic acid (FA) holds great potential as a convenient source of hydrogen for sustainable chemical synthesis and renewable energy storage. Herein, the non-noble metal nickel (Ni) exhibits superior promoting effect in improving the catalytic activity of Pd toward high activity and selectivity for FA decomposition at room temperature.

Formic acid (FA), as a major product of biomass processing, has attracted considerable attention as a potential hydrogen storage material due to its intrinsic advantages, including high hydrogen content, nontoxicity and easy recharging as a liquid (the availability of the existing infrastructure for gasoline and oil).[1,2] To maximize the efficacy of FA as a hydrogen storage material, one must follow the desired reaction pathway (HCOOH → CO_2 + H_2) and avoid the unwanted reaction (HCOOH → CO + H_2O).[3,4] So far, most of the attention on nanocatalysts (NCs) toward FA decomposition has been focused on noble metals, of which Au, Pt, and especially Pd exhibit excellent catalytic activity.[5] Unfortunately, monometallic Pd is still prone to deactivation due to the adsorption of poisonous carbon monoxide (CO) intermediates. Alloying with another metal, which holds superior CO anti-poisoning ability over Pd, seems to be a promising technique.[1d,2e,f] Thereafter, it is highly desirable to further increase the CO tolerance and catalytic performance of Pd NCs by integration of low-cost components.

Aside from tuning the catalyst composition, adjusting and optimizing the interaction between the active metal phase and the support materials are also key approaches to further improve catalytic performance.[6] Currently, graphene and carbon black are widely used as catalyst supports.[1b] However, the aggregation of graphene nanosheets (GNs) in aqueous solution and the weak interaction between carbon black (CB) and active metals still

limit further improvement in the performance of the catalyst.[7] Therefore, coupling the merits of both GNs and CB to enable the facile and effective synthesis of a well dispersed metal NC catalyst in aqueous solution and further discovering the intrinsically catalytic performances are highly desirable.

Herein, we advantageously combine Pd and Ni and use GNs–CB as a support to form PdNi/GNs–CB NCs, which exhibit excellent catalytic activity and hydrogen selectivity toward FA decomposition. Furthermore, PdNi@Pd/GNs–CB obtained *via* a substitution reaction between PdNi/GNs–CB and $PdCl^{4-}$ in aqueous solution exhibits enhanced cycle stability.

Fig. 1A shows the plots of the volume of generated gas (CO_2 + H_2) *versus* the reaction time during dehydrogenation of aqueous FA solution catalyzed by different catalysts. Clearly, the amount of gas generated from the FA decomposition over the Ni/GNs–CB catalyst is very small. In sharp contrast, compared to the Pd/GNs–CB catalyst, the PdNi alloy catalyst exhibits a much higher activity to complete the decomposition reaction of FA, indicating that Ni plays a critical role in improving the catalytic activity of Pd. Especially, when the atom ratio of Pd/Ni is 1/2, FA decomposes completely within only 35 min. Mass spectral profiles (Fig. S1, ESI†) show that no detectable amount of CO can be found in the gas mixture generated from the decomposition of FA. The reaction completeness is confirmed by the results of liquid chromatogram spectra (LC, $S_{before} \geq 2S_{after}$, Fig. S2, ESI†). In contrast, only ~70% of H_2 can be released from FA over Pd/GNs–CB even after 120 min,

[a] *State Key Laboratory of Rare Earth Resource Utilization, Changchun Institute of Applied Chemistry, Chinese Academy of Sciences, Changchun 130022, P. R. China. E-mail: xbzhang@ciac.ac.cn; Fax: +86 431-85262235; Tel: +86 431-85262235*
[b] *University of Chinese Academy of Sciences, Beijing, 100049, P. R. China.*
[c] *Changzhou Institute of Energy Storage Materials & Devices, Changzhou 213000, Jiangsu, China*
† Electronic supplementary information (ESI) available: Detailed synthesis conditions, experimental procedures, TEM characterization, XRD characterization, MS analyses of gas, LC characterization. See DOI: 10.1039/c3cc46248j
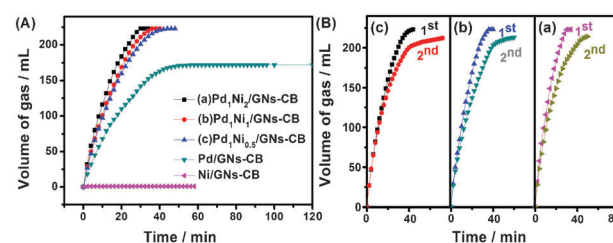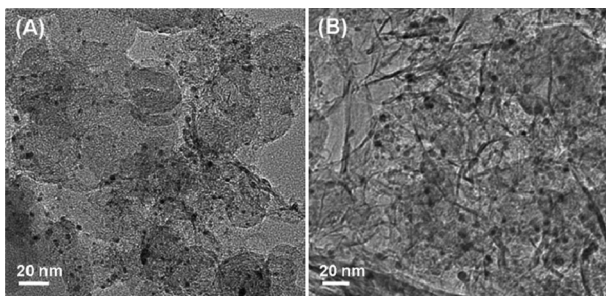

Fig. 1 (A) FA decomposition from 5 mL of aqueous FA (1 M HCOOH and 1 M HCOONa) and PdNi NCs with different atomic ratios of Pd/Ni. (B) Stability test of carbon supported PdNi catalyst from (A) (amount of catalyst: n_{Pd} = 0.067 mmol).

Fig. 2 TEM images of (A) Pd$_1$Ni$_2$/GNs–CB and (B) Pd/GNs–CB catalysts.

which is about more than 3 times worse than that over the PdNi/GNs–CB catalyst.

To confirm the elemental composition of the as-prepared catalysts, investigation using inductively coupled plasma atomic emission spectroscopy (ICP-AES) is carried out and the results are tabulated in Table S1 (ESI†). The transmission electron microscopy (TEM) images of PdNi and Pd loaded on GNs–CB are shown in Fig. 2A and B, where well dispersed NCs could be found clearly. Particle size distribution (Fig. S4, ESI†) derived from TEM images indicates that the addition of Ni decreases the particle size. From X-ray diffraction (XRD) patterns, it is seen that the Pd/GNs–CB exhibits the characteristics of a single face-centered-cubic crystallographic structure of Pd (Fig. S5, ESI,† PDF#46-1043). For Ni/GNs–CB, only the (111) peak could be found. Interestingly, the diffraction peaks of PdNi NCs are much weaker than those of Pd NCs, indicating that Ni addition can effectively restrain the growth of NCs, which is in accordance with the TEM results. It should be noted that the characteristic (111) peak of Pd in the PdNi/GNs–CB catalyst is shifted to higher 2θ values with respect to the corresponding peaks in the Pd/GNs–CB, indicating the formation of an alloy between Pd and Ni.

Considering that a smaller particle size of Pd results in even lower activity (rapid poisoning has been reported),[4b] the increase in catalytic performance might be attributed to its enhanced anti-poisoning ability to CO. The CO stripping voltammetry is then used as one useful probe to reflect the anti-poisoning ability of a noble metal surface toward CO.[5c] As is shown in Fig. 3A and B, it is interesting to note that both the onset potential (0.6 V for PdNi, 0.68 V for Pd) and the peak area of CO oxidation for the PdNi/GNs–CB are very low as compared with those for the Pd/GNs–CB catalyst, which indicates that the PdNi/GNs–CB catalyst possesses a strong capability of anti-poisoning to CO, which might be attributed to the change of the electronic state of Pd deriving from the electron-donating ability of Ni. In addition, as shown in Fig. 3C, Pd, Ni and C can be found. Compared to Pd/GNs–CB, the peak of Pd $3d_{5/2}$ shifts from 335.81 to 335.55 eV in PdNi/GNs–CB, indicating a slight electron transfer from Ni to Pd. This decreased binding energy of Pd 3d might change the chemisorption energy of the adsorbate[8,9] and thus might result in a weak CO interaction with the PdNi NCs.

Stability tests of carbon supported Pd–Ni catalysts are shown in Fig. 1B. It is found that the catalytic activities of all the catalysts undergo serious losses in the 2nd run. TEM images, ICP, and XRD are employed to understand the underlying mechanism of the instability of the PdNi catalysts. It is seen
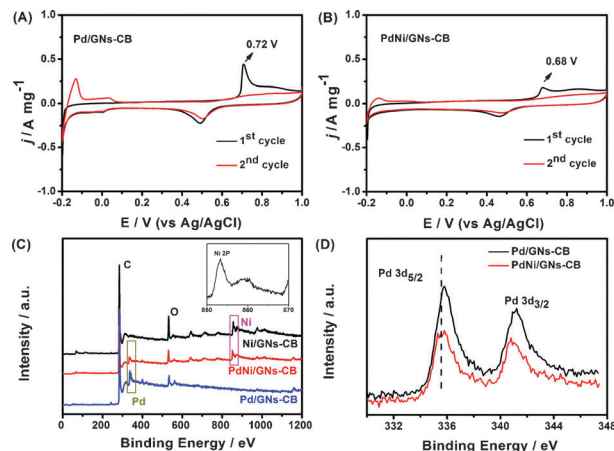

Fig. 3 CO stripping voltammograms on (A) Pd/GNs–CB and (B) PdNi/GNs–CB in 0.5 M H$_2$SO$_4$ solution at a scan rate of 50 mV s^{-1}. (C) Survey XPS spectroscopy of three kinds of catalysts. Inset: XPS spectrum for Ni 2P regions of PdNi/GNs–CB. (D) XPS spectrum for Pd 3d regions of Pd/GNs–CB and PdNi/GNs–CB.

from Fig. S3A (ESI†) that there is severe agglomeration of NCs after the reaction, and the average size of the nanoparticles also becomes bigger (Fig. S4, ESI†). During the catalytic process, Ni in the catalyst is easily eroded by H$^+$, which is consistent with the ICP results (Table S1, ESI†). Then the interaction between NCs and carbon supports becomes weak due to the erosion and results in a severe detachment and agglomeration of NCs (Fig. S5, ESI†). Thus, further investigations are needed to improve the durability of the present PdNi/GNs–CB catalyst.

To resolve the problem, Pd is employed to replace the Ni atom in the outer layers of the PdNi NCs to improve the stability of the structure as well as the stability of the catalysis. Interestingly, the as-synthesized PdNi@Pd/GNs–CB exhibits much enhanced catalytic activity and stability toward FA decomposition. Fig. 4A shows that 5 mL of FA decomposes completely in 10 min over PdNi@Pd/GNs–CB (TOF = 577 h^{-1}) which is higher than that over PdNi/GNs–CB (TOF = 529 h^{-1}). Inspired by the enhanced catalytic activity obtained from PdNi@Pd/GNs–CB, the cycle stability experiment is shown in Fig. 4B. Surprisingly, only a little degradation could be found during the experiments, performed 4 times, indicating that the PdNi@Pd/GNs–CB catalyst possesses good stability, which is supported by the TEM (Fig. S3B, ESI†), XRD (Fig. S5, ESI†), and ICP (Table S1, ESI†) results.

In summary, a facile method is used to synthesize well-dispersed PdNi NCs grown on a GNs–CB composite support to combine the advantages of GNs and CB. Unexpectedly, PdNi NCs loaded on GNs–CB exhibit higher catalytic performance for FA decomposition at room temperature in aqueous media than on Pd or Ni alone. Furthermore, Pd is employed to replace the surface Ni of PdNi NCs toward a novel PdNi@Pd catalyst to further improve the catalytic activity and stability. The use of GNs–CB as a new kind of carbon support to disperse, anchor, and further promote NCs with active components would undoubtedly assist long-term endeavours to further optimize and enhance the catalytic efficacy of catalysts in the development of FA as a hydrogen-storage material.
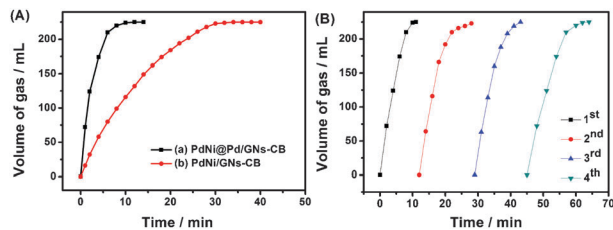
Fig. 4 (A) Plots of volume of CO_2/H_2 gas liberation over time from a stirred tank reactor containing 5 mL of aqueous FA (1 M HCOOH and 1 M HCOONa) and Pd-based catalyst (amount of catalyst: $n_{catalyst}$ = 0.2 mmol). (B) Four repeated tests of PdNi@Pd/GNs–CB.

Notes and references

1 (*a*) J. F. Hull, Y. Himeda, W. Wang, B. Hashiguchi, R. Periana, D. J. Szalda, J. T. Muckerman and E. Fujita, *Nat. Chem.*, 2012, **4**, 383; (*b*) J. Wang, X. B. Zhang, Z. L Wang, L. M. Wang and Y. Zhang, *Energy Environ. Sci.*, 2012, **5**, 6885; (*c*) Y. L. Qin, X. B. Zhang, J. Wang and L. M. Wang, *J. Mater. Chem.*, 2012, **22**, 14861; (*d*) O. Metin, X. Sun and S. Sun, *Nanoscale*, 2013, **5**, 910.
2 (*a*) W. Grochala and P. P. Edwards, *Chem. Rev.*, 2004, **104**, 1283; (*b*) L. Schlapbach and A. Zuttel, *Nature*, 2001, **414**, 353; (*c*) P. Chen, Z. Xiong, J. Luo, J. Lin and K. L. Tan, *Nature*, 2002, **420**, 302;

(*d*) H. L. Jiang, S. K. Singh, J. M. Yan, X. B. Zhang and Q. Xu, *ChemSusChem*, 2010, **3**, 541; (*e*) S. Zhang, Ö. Metin, D. Su and S. Sun, *Angew. Chem., Int. Ed.*, 2013, **52**, 3681; (*f*) Z. L. Wang, J. M. Yan, Y. Ping, H. L. Wang, W. T. Zheng and Q. Jiang, *Angew. Chem.*, 2013, **125**, 4502.
3 (*a*) M. Graseman and G. Laurenczy, *Energy Environ. Sci.*, 2012, **5**, 7854; (*b*) Q. Y. Bi, X. L. Du, Y. M. Liu, Y. Cao, H. Y. He and K. N. Fan, *J. Am. Chem. Soc.*, 2012, **134**, 8926; (*c*) X. Gu, Z. H. Lu, H. L. Jiang, T. Akita and Q. Xu, *J. Am. Chem. Soc.*, 2011, **13**, 11822; (*d*) D. A. Bulushev, L. Jia, S. Beloshapkin and J. R. H. Ross, *Chem. Commun.*, 2012, **48**, 4187; (*e*) F. Joó, *ChemSusChem*, 2008, **1**, 805.
4 (*a*) T. E. Springer, T. Rockward, T. A. Zawodzinski and S. Gottesfeld, *J. Electrochem. Soc.*, 2001, **148**, A11; (*b*) K. Tedsree, T. Li, S. Jones, C. W. A. Chan, K. M. K. Yu, P. A. Bagot, E. A. Marquis, G. D. W. Smith and S. C. E. Tsang, *Nat. Nanotechnol.*, 2011, **6**, 302.
5 (*a*) S. Jones, J. Qu, K. Tedsree, X. O. Gong and S. C. E. Tsang, *Angew. Chem., Int. Ed.*, 2012, **51**, 1; (*b*) X. Zhou, Y. Huang, C. Liu, J. Liao, T. Lu and W. Xing, *Chem. Commun.*, 2008, 3540; (*c*) Y. Huang, X. Zhou, M. Yin, C. Liu and W. Xing, *Chem. Mater.*, 2010, **22**, 5122; (*d*) S. W. Ting, S. Cheng, K. Y. Tsang, N. Van der laak and K. Y. Chan, *Chem. Commun.*, 2009, 7333; (*e*) Z. L. Wang, J. M. Yan, H. L. Wang, Y. Ping and Q. Jiang, *Sci. Rep.*, 2012, **2**, 598; (*f*) M. Yadav, T. Akita, N. Tsumori and Q. Xu, *J. Mater. Chem.*, 2012, **22**, 12582.
6 (*a*) A. Bruix, J. A. Rodriguez, P. J. Ramírez, S. D. Senanayake, J. Evans, J. B. Park, D. Stacchiola, P. Liu, J. Hrbek and F. Illas, *J. Am. Chem. Soc.*, 2012, **134**, 8968; (*b*) L. He, Y. Huang, A. Wang, X. Wang, X. Chen, J. J. Delgado and T. Zhang, *Angew. Chem., Int. Ed.*, 2012, **51**, 6191.
7 (*a*) C. Xu, X. Wang and J. Zhu, *J. Phys. Chem. C*, 2008, **112**, 19841; (*b*) F. Ye, X. Cao, L. Yu, S. Chen and W. Lin, *Int. J. Electrochem. Sci.*, 2012, **7**, 1251.
8 (*a*) B. Hammer and J. K. Nørskov, *Adv. Catal.*, 2000, **45**, 71; (*b*) J. Greeley, J. K. Nørskov and M. Maurikakis, *Annu. Rev. Phys. Chem.*, 2002, **53**, 319.
9 Z. Zhang, J. Ge, L. Ma, J. Liao, T. Lu and W. Xing, *Fuel Cells*, 2009, **9**, 114.